Shock Focussing Effect in Medical Science and Sonoluminescence
2003 Germany

3 Shock and Thermal Waves Emanating from a Sonoluminescing Gas Bubble

Ho-Young Kwak[1], Yoon-Pyo Lee[2]

[1]Mechanical Engineering Department, Chung-Ang University, Seoul, 156-756 Korea

[2]Korea Institute of Science and Technology, P.O. Box 131, Cheongryang, Seoul, 136-791 Korea

Abstract

The generation and propagation of the shock pulse from a sonoluminescing gas bubble whose wall acceleration reaches 10^{11} g near the collapse is considered by using the bubble wall motion developed by Keller and Miksis in conjunction with the analytical solutions for the gas inside bubble and the Kirkwood–Bethe hypothesis for the outgoing wave. The propagation of the pressure wave inside the bubble, where there are inhomogeneities of density, pressure and temperature induced by the rapid bubble collapse, is also treated. The propagation of a solition-like heat wave which is generated by "thermal spike" due to the rapid increase and subsequent decrease in the bubble wall acceleration is also discussed.

3.1 Introduction

The single-bubble sonoluminescence (SBSL) phenomenon which is the light emission from a trapped bubble under ultrasound near the collapse point has attracted considerable attention for its exotic characteristics. Recent experiments vitalized by the single-bubble levitation technique under ultrasound [9] have revealed that the light emission of SBSL is characterized by picosecond flashes of broad band spectrum which extends to ultraviolet [1, 13]. Also the bubble wall acceleration for SBSL has been found to exceed 10^{11} g at the instant of the collapse theoretically [28] and experimentally [42].

The gas temperature inside the bubble at near the collapse may be estimated from the spectrum of SBSL by assuming that the light source is black-body radiation [13], bremsstrahlung [18, 28] or the emission from the excited electrons confined inside the bubble [4]. The gas temperature fitted to the spectrums assumed are approximately in the range of 10 000 K $\sim$ 100 000 K and the gas pressure is estimated to be about 5000 $\sim$ 10 000 bar at the collapse.

However the mechanism of the light emission which has short pulse width and broad band spectrum cannot be explained adequately yet. Shock-induced emission for the sonoluminescence was suggested by Greenspan and Nadim [11]. Based on this argument, numerical simulations of the gas dynamics with the interior of the bubble were undertaken by Wu and Roberts [43], Moss et al. [34] and Kondic et al.[22]. In these models, without heat conduction inside the bubble an inwardly moving shock wave was found to be developed and reflected at the center to produce a very high temperature which is enough to emit light. However, the shock-wave model does not explain the ranges of ultrasound amplitude for which sonoluminescence (SL) can be observed [2] and the role of noble gas dopants for SL [14]. Furthermore, this model does not explain the observed bubble radii which can be taken into account by mass diffusion [31]. While Vuong and Szeri [41] have also reported that no development of steep shock inside the bubble is possible because of rapid diffusive transport. In their study, the gas dynamics inside the bubble features a wavy disturbance at an ultrasonic amplitude of 1.2 atm or greater. Recently, an alternative mechanism for the SL was suggested [28]. The light emission occurs in consequence of the "thermal spike" induced by the rapid increase and subsequent decrease in the bubble-wall acceleration, whose maximum value exceeds 10^{12} m/s^2 near the collapse [29]. Anyway, the problem of whether a shock or pressure wave is formed inside the bubble is a fundamental problem in the study of sonoluminescence.

In this study the pressure wave propagation inside the bubble and the outward shock propagation from the bubble wall was investigated theoretically by using the bubble-wall motion developed by Keller and Miksis [20] in conjunction with the analytical solutions for the Navier–Stokes equations with spherical symmetry [29] and the Kirkwood–Bethe hypothesis [21]. Also, the heat diffusion from the sonoluminescing bubble, which produces a high temperature and pressure environment adjacent to the bubble wall, was considered by solving the heat diffusion equation numerically.

3.2 Bubble Dynamics

3.2.1 A Model of Bubble Oscillation Under Ultrasound

A bubble dynamics model suggested by Ryu and Kwak [38] was employed for the consideration of the growth and collapse of a bubble under ultrasound. A sketch of the bubble model used is given in Fig. 3.1, which shows a spherical air bubble in liquid at ambient temperature, T_∞ and ambient pressure P_∞.

Mass transfer through the bubble interface and evaporation or condensation of water molecules at the interface are not considered in this analysis. Heat transfer is assumed to occur through the thermal boundary layer having thickness $\delta(t)$. The temperature profile in this analysis is assumed to be quadratic and as follows [40]:

$$\frac{T - T_\infty}{T_{\mathrm{bl}} - T_\infty} = (1 - \zeta)^2 \qquad (3.1)$$

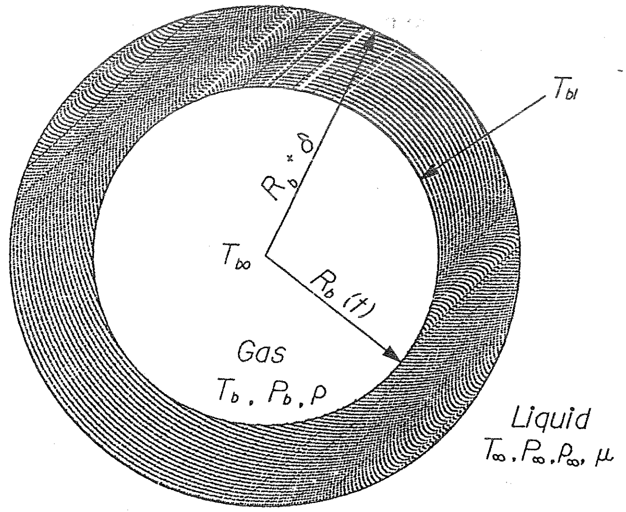

Fig. 3.1. A physical model with thermal boundary layer for the forced oscillation of a spherical bubble in liquid under an ultrasonic field

where $\zeta = \frac{r-R_b}{\delta}$, T_{bl} is the temperature at the bubble wall, and R_b is the instantaneous bubble radius. Such a second-order curve satisfies the following boundary conditions used in this model:

$$T(R_b, t) = T_{bl}, \tag{3.2}$$

$$T(R_b + \delta, t) = T_\infty, \tag{3.3}$$

$$\left(\frac{\partial T}{\partial r}\right)_{r=R_b+\delta} = 0. \tag{3.4}$$

The bubble model with such a liquid-phase reaction zone has been verified experimentally [39].

3.2.2 Density, Velocity and Pressure Profiles for the Gas Inside the Bubble

First, consider the mass and momentum equations whose analytical solutions with spherical symmetry exist. The equations are given by

$$\frac{\partial \rho_g}{\partial t} + \frac{1}{r^2}\frac{\partial}{\partial r}(\rho_g u_g r^2) = 0, \tag{3.5}$$

$$\frac{\partial}{\partial t}(\rho_g u_g) + \frac{1}{r^2}\frac{\partial}{\partial r}(\rho_g u_g^2 r^2) + \frac{\partial P_b}{\partial r} = 0, \tag{3.6}$$

where r is the distance from the bubble center, ρ_g is the density of the gas and u_g is the gas velocity, which obeys $u_g(R_b, t) = U_B$. The solutions satisfying

(3.5) and (3.6) with an assumption of the linear velocity profile given in (3.8) have been obtained by Kwak and Yang [27]. These are given as

$$\rho_g = \rho_0 + \rho_r, \tag{3.7}$$

$$u_g = \frac{\dot{R}_b}{R_b} r, \tag{3.8}$$

$$P_b = P_{b0} - \frac{1}{2}(\rho_0 + \frac{1}{2}\rho_r)\frac{\ddot{R}_b}{R_b} r^2, \tag{3.9}$$

where $r_0 R_b^3 = const.$, $\rho_r = ar^2/R_b^5$ and the dot denotes the time derivative. The constant a is related to the mass of the gas inside the bubble as

$$\frac{a}{m} = \frac{5}{4\pi}(1 - N_{BC}), \tag{3.10}$$

where $N_{BC} = (P_{b0}R_b^3/T_{b0})/(P_\infty R_e^3/T_\infty)$, T_{b0} and P_{b0} are the gas temperature and pressure at the bubble center, respectively, and R_e is the equilibrium radius. The velocity profile obtained shows the homologous character of the gas inside the bubble, which is encountered in gravitational collapse [19]; every mass point during the collapse or expansion may be traced back to a single point, the center of bubble. It is noted that the stress terms in the momentum equation as well as the viscous dissipation terms in the energy equation vanish for the spherical symmetry case.

One could check that the solutions given in (3.7)–(3.9) satisfy the mass and momentum conservations at hand. Until the characteristic time of the bubble evolution is much less than the relaxation time of the translational motion of the gas molecules inside the bubble, the uniform pressure approximation is legitimate [26, 27].

3.2.3 Bubble Wall Motion

The instantaneous bubble radius and bubble-wall velocity which are needed in the study of bubble behavior have been obtained by the equation from the Keller and Miksis formulation [20]. This equation, which includes the effects of liquid compressibility, is

$$\left(1 - \frac{U_b}{C_B}\right) R_b \frac{dU_b}{dt} + \frac{3}{2}U_b^2\left(1 - \frac{U_b}{3C_B}\right) = \frac{1}{\rho_\infty}\left(1 + \frac{U_b}{C_B} + \frac{R_b}{C_B}\frac{d}{dt}\right)\left[P_B - P_S\left(t + \frac{R_b}{C_B}\right) - P_\infty\right], \tag{3.11}$$

where R_b is the radius of the bubble, U_b is the velocity of the bubble, C_B is the speed of sound in the liquid at the bubble wall and ρ_∞ is the density of the medium. The liquid pressure on the wall of the bubble P_{B} is related to the pressure inside the bubble wall P_{b} by

$$P_{\mathrm{B}} = P_{\mathrm{b}} - 2\sigma/R_{\mathrm{b}} - 4\mu U_{\mathrm{b}}/R_{\mathrm{b}}. \tag{3.12}$$

The pressure of the driving sound field P_{S} may be represented by a sinusoidal function such as

$$P_{\mathrm{S}} = -P_{\mathrm{A}} \sin \omega t, \tag{3.13}$$

where P_{A} is the driving sound amplitude. The bubble wall velocity U_{b} is just the time derivative of the bubble radius, i.e.

$$\frac{\mathrm{d}R_{\mathrm{b}}}{\mathrm{d}t} = U_{\mathrm{b}}. \tag{3.14}$$

Essentially, (3.11) is the acoustic approximation and is quite good until the bubble-wall velocity is comparable to the speed of sound in the liquid. The equation for the bubble-wall motion based on the acoustic approximation can also be derived from the unsteady Bernoulli equation for irrotational flow and the linearized wave equation with an appropriate boundary condition [44].

3.2.4 Temperature Distribution Inside the Bubble

The continuity equation, the momentum equation with Newton's viscous law and an energy equation with Fourier's conduction law are commonly referred as the Navier–Stokes equations [36]. Now, to solve the Navier–Stokes equations is to find the solution for the energy equation. A procedure to obtain the solution for the energy equation in which the viscosity dissipation terms vanish because of the spherical symmetry is as follows.

Assuming that the internal energy of the gas inside the bubble is a function only of the gas temperature as given by $\mathrm{d}e = C_{\mathrm{v,b}}\mathrm{d}T_{\mathrm{b}}$, where $C_{\mathrm{v,b}}$ is the constant volume specific heat, the energy equation becomes

$$\rho_{\mathrm{g}} C_{\mathrm{v,b}} \frac{\mathrm{D}T_{\mathrm{b}}}{\mathrm{D}t} = -\frac{P_{\mathrm{b}}}{r^2}\frac{\mathrm{d}}{\mathrm{d}r}(r^2 u_{\mathrm{g}}) - \frac{1}{r^2}\frac{\mathrm{d}}{\mathrm{d}r}(r^2 q_{\mathrm{r}}), \tag{3.15}$$

where q_{r} is the radial component of the heat flux inside the bubble. Since the solutions given in (3.7)–(3.9) also satisfy the kinetic energy equation, only (3.15) remains to be solved. With help of the enthalpy representation of the energy equation, one can eliminate $\mathrm{D}/\mathrm{D}t = (\partial/\partial t + u_{\mathrm{g}}\partial/\partial r)T_{\mathrm{b}}$ to obtain

$$\frac{\mathrm{D}P_{\mathrm{b}}}{\mathrm{D}t} = -\frac{\gamma P_{\mathrm{b}}}{r^2}\frac{\mathrm{d}}{\mathrm{d}r}(r^2 u_{\mathrm{g}}) - \frac{\gamma - 1}{r^2}\frac{\mathrm{d}}{\mathrm{d}r}(r^2 q_{\mathrm{r}}). \tag{3.16}$$

The flash of SL emitted just before the bubble collapse may be closely related to the acceleration of the bubble wall. Taking into account the bubble-wall acceleration, given in (3.9), from (3.7)–(3.9) and (3.16), we obtain

$$\frac{\gamma-1}{r^2}\frac{\mathrm{d}}{\mathrm{d}r}(r^2 q_r) = \tag{3.17}$$
$$-\left[\frac{\mathrm{d}P_{\mathrm{b}0}}{\mathrm{d}t}+3\gamma P_{\mathrm{b}0}\frac{\dot{R}_{\mathrm{b}}}{R_{\mathrm{b}}}\right]+\frac{1}{2}\left(\rho_0+\frac{1}{2}\rho_r\right)\left[(3\gamma-2)\frac{\dot{R}_{\mathrm{b}}\ddot{R}_{\mathrm{b}}}{R_{\mathrm{b}}^2}+\frac{\dddot{R}_{\mathrm{b}}}{R_{\mathrm{b}}}\right]r^2.$$

The solution of the above equation can be obtained by the superposition of the contribution from the uniform and radially dependent pressure distributions such as

$$T(r) = T_{\mathrm{b}}(r) + T_{\mathrm{b}}'(r), \tag{3.18}$$

where the temperature profile $T_{\mathrm{b}}(r)$ is the solution of the following energy equation with uniform pressure inside bubble:

$$\frac{(\gamma-1)}{r^2}\frac{\mathrm{d}}{\mathrm{d}r}(r^2 q_0) = -\left[\frac{\mathrm{d}P_{\mathrm{b}0}}{\mathrm{d}t}+3\gamma P_{\mathrm{b}0}\frac{\dot{R}_{\mathrm{b}}}{R_{\mathrm{b}}}\right]. \tag{3.19}$$

Assuming the conductivity for the gas inside the bubble as $k_{\mathrm{g}} = AT + B$, one may obtain the temperature distribution from (3.19). It is

$$T_{\mathrm{b}}(r) = \frac{B}{A}\left[-1+\sqrt{\left(1+\frac{A}{B}T_{\mathrm{b}0}\right)^2 - 2\eta\frac{A}{B}(T_{\mathrm{bl}}-T_\infty)\left(\frac{r}{R_{\mathrm{b}}}\right)^2}\,\right], \tag{3.20}$$

where $\eta = \frac{R_{\mathrm{b}}}{\delta}\frac{k_{\mathrm{l}}}{B}$ and k_{l} is the thermal conductivity of the liquid. The thickness of the thermal boundary layer δ adjacent to the bubble wall may be determined from the mass, momentum and energy equations for the liquid with the assumption of a quadratic temperature profile in that zone. Applying the integral method to the energy equation of the liquid in the layer, one may obtain the time-dependent equation for the layer thickness [38] as

$$\left[1+\frac{\delta}{R_{\mathrm{b}}}+\frac{3}{10}\left(\frac{\delta}{R_{\mathrm{b}}}\right)^2\right]\frac{\mathrm{d}\delta}{\mathrm{d}t} = \tag{3.21}$$
$$\frac{6\alpha}{\delta}-\left[\frac{2\delta}{R_{\mathrm{b}}}+\frac{1}{2}\left(\frac{\delta}{R_{\mathrm{b}}}\right)^2\right]\frac{\mathrm{d}R_{\mathrm{b}}}{\mathrm{d}t}-\delta\left[1+\frac{\delta}{2R_{\mathrm{b}}}+\frac{1}{10}\left(\frac{\delta}{R_{\mathrm{b}}}\right)^2\right]\frac{\mathrm{d}T_{\mathrm{bl}}}{\mathrm{d}t}/(T_{\mathrm{bl}}-T_\infty).$$

Such an ordinary differential equation for δ is very convenient to study the chaotic behavior of the bubble and the SL phenomenon, which needs enormous computing time to simulate. The solution given by (3.20) indicates that the temperature distribution of the gas inside the bubble is solely determined by the conduction heat transfer, which is perfectly valid for the nonsonoluminescing gas bubble. It is noted that the temperatures at the bubble center and at the wall are determined from the values of T_{b0}, T_{bl} and $\dot{R}_b$ in the near past by the Runge–Kutta method [27].

An abrupt rise in temperature and the subsequent rapid quenching due to the bubble-wall acceleration and the increase and decrease in the acceleration may be treated on another timescale [7], different from the bubble motion described by (3.19). A solution of the nonuniform pressure part in (3.17), which is the temperature profile with respect to the heat flux $(q - q_0)$, with the assumption of no temperature gradient at the bubble center is given by

$$T_b'(r) = -\frac{r^4}{40(\gamma-1)k_g'}\left(\rho_0+\frac{5}{21}\rho_r\right)\left[(3\gamma-2)\frac{\dot{R}_b\ddot{R}_b}{R_b^2}+\frac{\dddot{R}_b}{R_b}\right]+C. \qquad (3.22)$$

The coefficient C may be determined from the boundary condition $k_g' \mathrm{d}T_b/\mathrm{d}r = k_l \mathrm{d}T_l/\mathrm{d}r$ at the bubble wall, where $T_l(r)$ is the linear temperature profile at the thermal boundary layer with thickness δ', and is given by

$$C = \frac{1}{20(\gamma-1)}\cdot\left[(3\gamma-2)\dot{R}_b\ddot{R}_b R_b + \dddot{R}_b R_b^2\right] \qquad (3.23)$$

$$\times\left[\frac{\delta'}{k_l}\left(\rho_0+\frac{5}{14}\rho_{r=R_b}\right)+\frac{R_b}{2k_g'}\left(\rho_0+\frac{5}{21}\rho_{r=R_b}\right)\right].$$

The gas conductivity at ultra-high temperatures may be obtained from collision integrals [5] and the boundary layer thickness δ' may be chosen so that a proper bouncing motion results after the collapse [29]. The temperature distribution from (3.20) may be regarded as a background one, because the thermal spike represented by (3.22) is so short, being less than 500 ps. The temperature distribution given by (3.22) is appreciable when the bubble-wall acceleration reaches 10^{12} m/s^2, which occurs just prior to the 500 ps before the collapse. During the bubble evolution of every cycle except the collapsing period of 500 ps, the temperature distribution inside the bubble is determined by (3.20). The sharp increase in the temperature due to the rapid change of the bubble-wall velocity may happen because the change in the kinetic energy converts into heat when the kinetic energy of the gas inside the bubble decreases [45]. The unknown five variables $P_b, U_b, R_b, T_b(r)$ and δ for the background temperature profile inside the bubble may be obtained from five equations such as (3.9), (3.11), (3.14), (3.20) and (3.21), respectively. U_b and P_b are sufficient to provide the initial data for the calculation of the shock emission from the collapsing bubble. The solution given in (3.22) and (3.23) results in the generation of a thermal spike due to the sudden increase and subsequent decrease in the bubble-wall acceleration near the bubble collapse [28].

Recently the concept of a finite response time of the bubble to the external driving force has been suggested [24]. In general, the characteristic frequency of the driving force f_0 differs from the natural frequency of the bubble oscillation $1/t_0$. With these two characteristic frequencies related to the bubble oscillation under ultrasound, the retarded time of the bubble motion with respect to the external force may be defined as [24]

$$\tau = 1/f_0 - t_0. \tag{3.24}$$

Since the natural frequency of the bubble oscillation $1/t_0$, as can be seen in (3.3), is inversely proportional to the equilibrium radius R_0, the retarded time of the bubble motion depends also on the radius. In fact, it has been observed that the characteristic ratio of the maximum bubble radius to the equilibrium radius R_0 decreases as R_0 increases for a sonoluminescing gas bubble in the air–water system [10], which suggests that the response time of the bubble motion under ultrasound may depend on the equilibrium radius.

3.3 Shock Propagation from Collapsing Bubble

3.3.1 Characteristics of the Shock Wave

The rapidly collapsing bubble with a bubble-wall acceleration above 10^{11} g [28, 47] may emit shock waves from the bubble center in the outward direction (implosion). The velocity and the pressure fields in the liquid, caused by the shock waves originating from the rapidly collapsing bubble wall, may be obtained by using the Kirkwood–Bethe hypothesis. The hypothesis assumes that the invariant quantity Y, which is the following equation (3.25), propagates in the medium with the characteristic velocity, $c + u$:

$$Y = r\left(h + \frac{u^2}{2}\right) = R_\mathrm{b}\left(H_\mathrm{b} + \frac{U_\mathrm{b}^2}{2}\right). \tag{3.25}$$

The ordinary differential equations for the velocity and pressure of the outgoing characteristics are as follows [21]:

$$\left(\frac{\mathrm{d}u}{\mathrm{d}t}\right)_\mathrm{char} = \frac{1}{c-u}\left[(c+u)\frac{Y}{r^2} - \frac{2c^2u}{r}\right], \tag{3.26}$$

$$\left(\frac{\mathrm{d}p}{\mathrm{d}t}\right)_\mathrm{char} = \frac{\rho_\infty}{r(c-u)}\left(\frac{p+B'}{p_\infty+B'}\right)^{1/n}\left[2c^2u^2 - \frac{c(c+u)}{r}Y\right], \tag{3.27}$$

where the propagation velocity of the shock wave is given by

$$\frac{\mathrm{d}r}{\mathrm{d}t} = c + u. \tag{3.28}$$